Extreme space weather events of solar cycle 24: X-class solar flares and their impact on the low-latitude D-region ionosphere

K. Venkatesham[1,3], Ajeet K. Maurya[2,*], Rajesh Singh[1] and Suneet Dwivedi[3]

[1]KSK Geomagnetic Research Laboratory, Indian Institute of Geomagnetism, Prayagraj 211 506, India
[2]Department of Physics, Babasaheb Bhimrao Ambedkar University, Lucknow 226 025, India
[3]K. Banerjee Centre of Atmospheric and Ocean Studies, University of Allahabad, Prayagraj 221 002, India

X-class solar flares, which occurred in the daytime from 2008 to 2016 during solar cycle 24, were studied for their influence on the lower ionosphere over the low-equatorial Indian region. To understand the D-region behaviour during flare events, we used the very low frequency (VLF) navigational transmitter NWC (19.8 kHz) signal recorded at Pryagraj, Uttar Pradesh, India. A total of seven parameters were estimated: (i) the magnitude of X-ray flux, (ii) VLF signal rising amplitude perturbation (SRAP), (iii) X-ray flux and NWC signal start time difference (STD), (iv) peak time difference (PTD), (v) Wait's ionospheric parameters h' (reference height), (vi) β (sharpness factor) and (vii) D-region electron density difference (EDD) to determine the overall effect of solar flares on the D-region. The results suggest that three parameters (X-ray flux, SRAP and h') show a decreasing trend through the linear fit line, two parameters (β and EDD) show an increasing trend, while the remaining two parameters show a mixed trend (decrease during low activity and increase during high activity). Further, the trend line during the diurnal variation shows an increasing trend for X-ray flux, PTD and h', and a decreasing trend for SRAP, STD, β and EDD. Deviation in the case of individual events may indicate the dependence of these parameters on the seasons as well. The present study will provide the base for more robust analysis and modelling work in the future to understand the complexity of ionospheric change during flare events, and to develop a predictive model for space weather mitigation.

Keywords: D-region ionosphere, space weather, solar cycle, solar flares, trend line, VLF waves.

THE D-region is the lowest region of the Earth's ionosphere (altitude: 60–90 km), also known as the lower ionosphere, with minimum electron density (~10^3 el/cm^3). It acts as a sandwich region between the Earth's neutral atmosphere (mesosphere) and ionized atmosphere (ionosphere) and hence plays a significant role in the overall Sun–Earth relationship. Disturbances from above (e.g. solar flares, solar eclipse) and below (e.g. thunderstorm, lightning) the D-region affects it and controls its dynamics. Technically, this region is also important for radio-wave propagation; it reflects, propagates and absorbs radio waves depending on the wave frequency and electron density in this region[1]. Overall the D-region is one of the central layers for many important space weather and climate processes but remains poorly understood due to its low altitude and electron density[2–5].

It is well known that very low frequency (VLF; 3–30 kHz) radio signals generated from lightning discharges[6] and human-made navigational transmitters are cost-effective for continuously monitoring the D-region ionosphere[7–9]. Solar flares are grouped into different classes, namely A (10^{-8}–10^{-7} W/m^2), B (10^{-7}–10^{-6} W/m^2), C (10^{-6}–10^{-5} W/m^2), M (10^{-5}–10^{-4} W/m^2) and X (>10^{-4} W/m^2) depending on the X-ray peak flux in the range 1–8 Å as measured by the X-ray instrument on-board the geostationary environmental operational satellite (GOES)[10]. The flares perturb the entire daytime ionosphere[11], but their effect is more pronounced in the D-region[11,12]. During a solar flare event, the increased X-ray flux from the sun in the wavelength range 1–8 Å ionizes the major D-region constituents, viz. O_2 and N_2, along with neutrals at 60–75 km altitude[1,11]. Such a large increase in the D-region ionization modifies its properties, mainly conductivity and electron density, and also affects the VLF signal propagation conditions and appears as an anomaly in the VLF signal[13]. The effects of solar flares on the D-region and hence on the VLF signal vary with the class of a solar flare and are highest for the X-class flare[14]. Further, the effects on the ionosphere also depend on several parameters such as the location of flares on the solar disk, solar zenith angle, geographic location, season and phase of solar activity[15,16].

The X-class flares are the strongest of all classes due to their highest X-ray irradiance (>10^{-4} W/m^2) flux, and this affects the D-region maximally. A statistical study was performed in the Indian region by taking one year of flare events (including all flares from C to X from 2010 to 2011)[5]. Comparative studies were done between the changes in VLF anomalies and time delay with respect to solar X-ray flux with special emphasis on the local time dependence

*For correspondence. (e-mail: ajeet.iig@gmail.com)

of the flare events[17,18]. Many other studies in the past were based on the effect of a single X-class flare event only[19].

The present study from the Indian low-latitude region takes into account X-class solar flares of solar cycle 24 which occurred during daytime from 2008 to 2016. Since the ionospheric response to solar flares is different even for the same class depending on the local time, season and phase of the solar cycle, a detailed study considering several X-class flares covering a full solar cycle is required in order to understand the effect of the strongest flare event on the lower (D-region) ionosphere in the low-latitude region. To the best of our knowledge, there are no studies till date on the comparative effect of several X-class flares on the D-region of the ionosphere from the Indian low-latitude region.

Experimental set-up and data

The VLF data recorded at low-latitude station Pryagraj (formerly Allahabad; 25.4°N lat., 81.93°E long.), Uttar Pradesh, India, using a VLF receiver (AWESOME) was used in this study[20–22]. The amplitude data from NWC VLF navigational transmitter was used in the analysis. Figure 1 shows the location of the receiving station Pryagraj and NWC (19.8 kHz, 21.82°S lat., 114.17°E long.) VLF transmitter from Australia, along with their transmitter receiver great circle paths (TRGCPs). The NWC–Pryagraj TRGCP lies in the low-equatorial latitude region with a path length of ~6400 km (ref. 21). Mainly, amplitude data were used for detailed analysis because the phase data were poor for all the flare events.

In order to accurately extract the D-region parameter changes during the solar flare events, we have used long wave propagation capability (LWPC) modelling code[23]. This code provides two characteristic parameters: reference height h' (km) and electron density sharpness factor β (km^{-1}), also known as Wait's lower ionospheric parameters. The electron density is calculated using the following equation[24]

$$N_e(z) = 1.43 \times 10^7 \times (\exp(-0.15h')\exp(\beta - 0.15)(z - h')) \text{ cm}^{-3}, \quad (1)$$

where $N_e(z)$ is the electron density as function of altitude z.

We have analysed daytime (India LT = UT + 5.5 h) X-class solar flares, which occurred during solar cycle 24. Figure 2 shows solar Lyman-α flux (10^{-3} W/m^2) (green line) as a proxy for the behaviour of solar cycle 24. The Lyman-α flux was smoothed using the Savitzky–Golay filter with 128 days window length. The Lyman-α flux data were obtained from the Laboratory for Atmospheric and Space Physics (LASP) Data Center, USA (http://lasp.colorado.edu/lisird/lya/). In Figure 2, the daytime X-class flares which occurred after 2008 are shown by squares. In total, 18 X-class solar flares occurred during the daytime of TRGCP. Further, depending on the NWC VLF data quality and availability, only nine solar flares were considered for analysis (stars, Figure 2). Thus, the analysed solar flares (stars) cover the extreme solar activity from 2011 up to 2016.

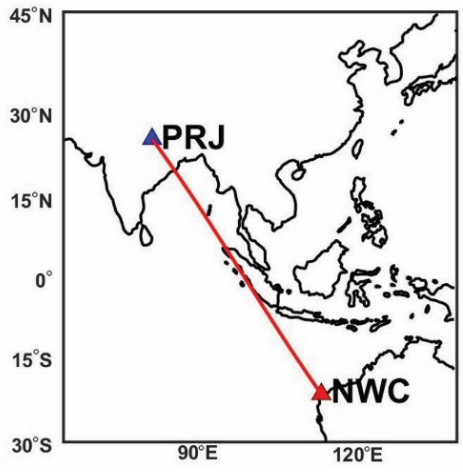

Figure 1. Location of NWC transmitter signal received at low-latitude Indian station Pryagraj (PRJ), Uttar Pradesh, India.

Observations

Effect of solar X-class flares on NWC VLF signal

Figure 3 shows example plots of well-defined X-class flares on NWC VLF data during the morning, noon and evening. The left panel in Figure 3 *a* shows the X-class flare perturbation on the NWC VLF signal amplitude (blue colour) recorded at Pryagraj on 23 October 2012 at 03:19 UT in the morning time. The middle and right panels in Figure 3 *a* show noon and evening time perturbations on 19 October 2014 at 05:00 UT and 9 August 2011 at 08:06 UT respectively. The corresponding X-ray flux from the GOES satellite is also shown (solid line) on each representative day. The two vertical lines (solid and dotted) just before the solar flare represent the onset time of the X-ray flare and NWC VLF amplitude perturbation respectively. Figure 3 *b* shows the corresponding phase data. As expected, the VLF signal amplitude significantly increases compared to normal unperturbed time. The time evolution of the D region height variation during each flare is significant as it affects the E region densities indirectly and the electrojet current system. So we have also added the D-region height variation with time (Figure 3 *b*). The D-region height in all three cases decreases as the flare effect increases. As suggested by Grubor *et al.*[14], a mirror type of reflection is required for such an increase in the VLF signal amplitude. X-class flares are the strongest; hence it is interesting to know how their effects vary with local time, season and phase of the solar cycle. Table 1 presents details of all X-class solar flares considered in the present study.

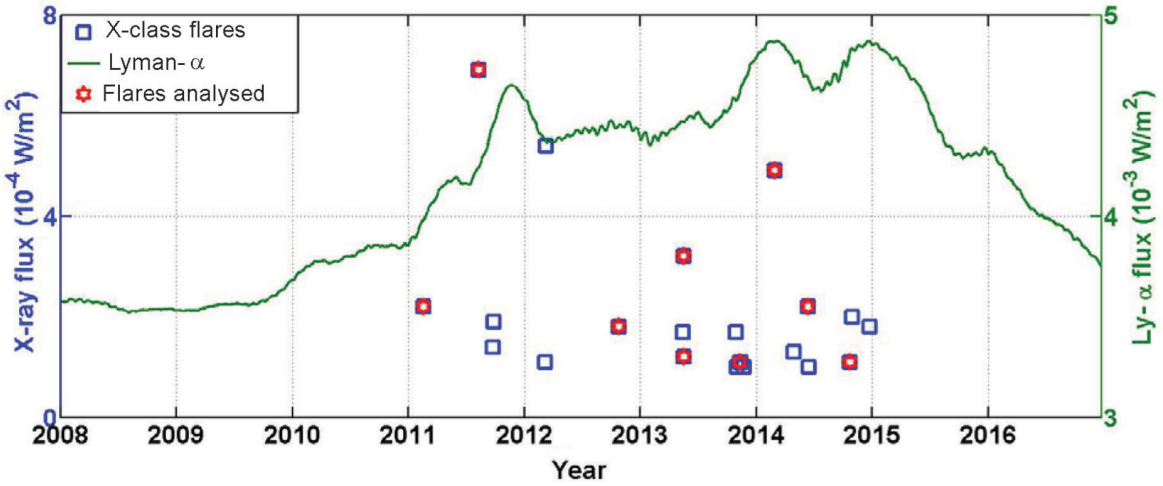

Figure 2. Lyman-α flux (128 days smoothed time variation) as a proxy of solar cycle 24 from 2008 to 2016. Squares are the X-class solar flares which occurred during this period, while stars are the X-class solar flares analysed in this study.

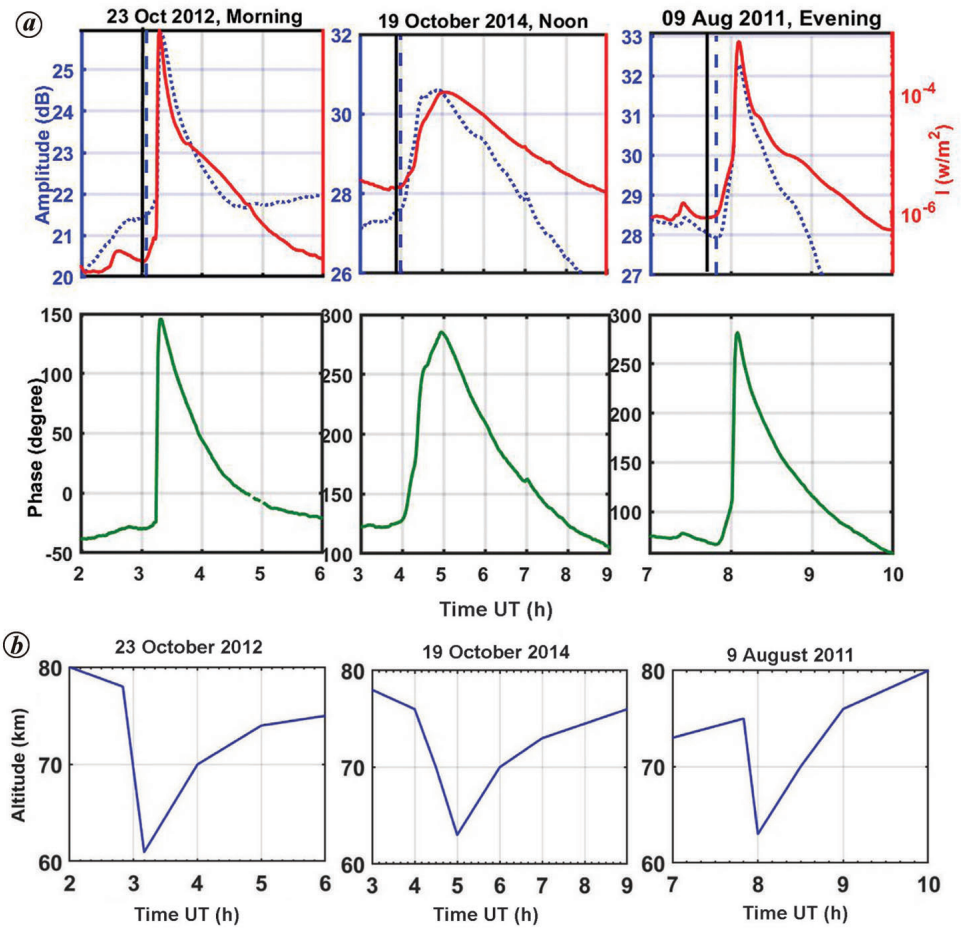

Figure 3. ***a***, Representative X-class solar flares during morning, noon and evening. Dotted line is the NWC amplitude and solid line is the X-ray flux. The two vertical lines (dotted and solid) are the start time of X-class solar flare and its effect on the VLF signal respectively. ***b***, NWC phase variation for the respective flares. Time evolution of the D-region altitude during flare events is also shown.

We have estimated the following flare parameters: (1) Magnitude of the X-ray flux. (2) NWC signal rising amplitude perturbation (SRAP), which is the difference between VLF amplitude at peak time minus VLF amplitude at onset time of flare perturbation in the VLF signal. (3) X-ray flux and NWC signal start time difference (STD) which is the

Table 1. Selected all X-class flares

Flare class	Flare time (UT)	Amplitude diff (ΔA)	Relaxation time ($\Delta\tau$)	Flare date
X 6.9	08:06	4.19 dB	1 min	2011-08-09
X 4.9	00:56	7.76 dB	6 min	2014-02-25
X 3.2	01:13	7.49 dB	1 min	2013-05-14
X 2.2	01:57	6.97 dB	0 min	2011-02-15
X 1.8	03:19	3.92 dB	1 min	2012-10-23
X 1.2	01:48	6.08 dB	1 min	2013-05-15
X 1.1	04:27	2.95 dB	0 min	2013-11-08
X 1.1	05:03	5.38 dB	4 min	2014-10-19
X 1.0	09:07	4.26 dB	0 min	2014-06-11

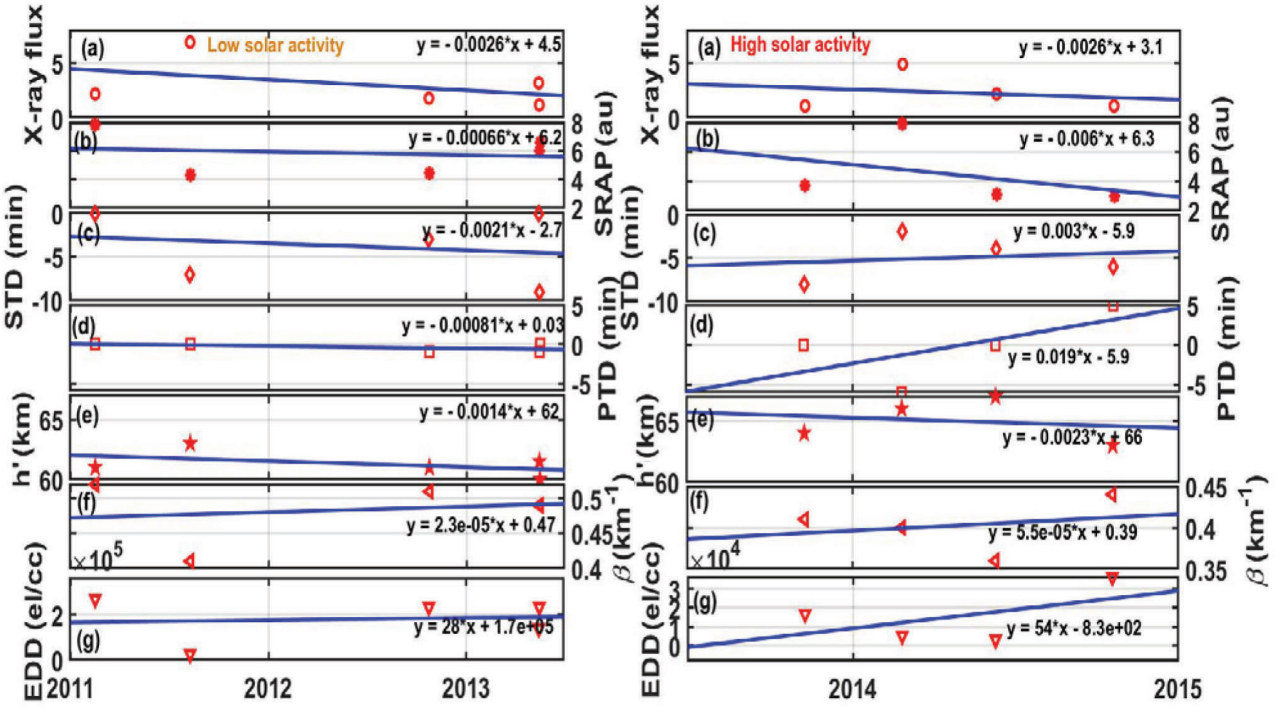

Figure 4. (Left panel) Low solar activity (during 2011–mid-2013) variation of (a) X-ray flux (left y-axis), (b) SRAP, (c) STD, (d) PTD, (e) h', (f) β and (g) EDD parameters. (Right panel) High solar activity (during mid-2013–2015) variation of (a) X-ray flux (left y-axis), (b) SRAP, (c) STD, (d) PTD, (e) h', (f) β and (g) EDD parameters. The linear fit line shows the trend of variation along with the fit equation.

difference between NWC signal onset time and X-ray flux onset time. (4) Peak time difference (PTD) which is the difference between NWC signal amplitude peak time and X-ray flux peak time also called 'relaxation time'[11]. Wait parameters, viz. (5) h' (reference height), (6) β (sharpness factor) and (7) electron density difference (EDD) were also determined to understand the overall effect of solar flares on the lower ionosphere/D-region.

It should be noted that we analysed only nine daytime X-class flare events during the period 2011–16. This number is small to provide any dependency on the solar cycle, diurnal and seasonal variations. However, X-class flares are rare, especially when we consider only daytime events; their number is further reduced. Hence, the present study is important from the VLF data and space weather analysis from the Indian low-latitude region.

Solar flare parameter variations during high and low solar activity

In order to understand, the effect of X-class flares on the D-region during various phases of a solar cycle, we have divided the analysis into two periods (low and high) of solar activity. The solar flare events considered in this study occurred during 2011–15. According to the Lyman-α variation in Figure 1 and sunspot number (not shown here), the above period is divided into low solar activity (during 2011 to mid-2013) and high solar activity (during mid-2013 to 2015). Figure 4 shows variations of the different parameters. The linear fit line along with equations $y = mx + c$ is also shown.

Figure 4a (left and right panels) depicts the X-ray flux ($\times 10^4$ W/m^2) of solar flare events for low and high solar

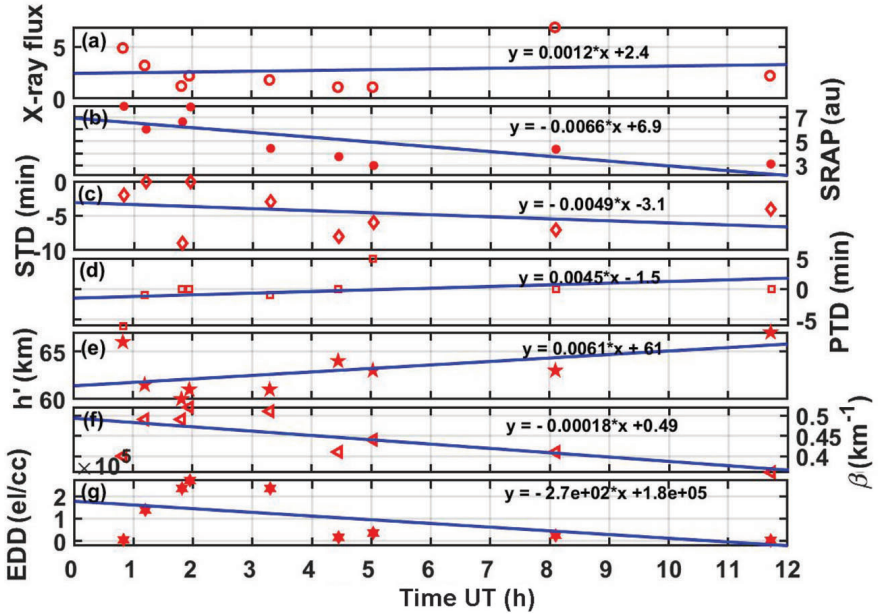

Figure 5. Diurnal variation of (a) X-ray flux, (b) SRAP, (c) STD, (d) PTD, (e) h', (f) β and (g) EDD parameters. The linear fit line shows the trend of variation along with the fit equation.

activity periods respectively, of solar cycle 24. The linear fit line shows a decreasing trend, which is supported by a negative slope from the fit equations in both the left and right panels. For SRAP (Figure 4b left and right panels), the linear fit line shows a decreasing trend during both low and high solar activity periods, but a greater slope during high activity period. STD (Figure 4c left and right panels) shows a decreasing trend during low activity period and an increasing trend during high activity period. PTD (Figure 4d left and right panels) follows a similar trend of decrease and increase as that of STD. Further, the minimum and maximum values of PTD vary between 0 and 6 min. The Wait's parameter h' (Figure 4e left and right panels) closely follows the variation trend of X-ray flux, i.e. the linear fit line shows decreasing trend during both low and high solar activity periods. The h' values during low solar activity period are lower (between ~62.0 and 60.7 km) than those during high solar activity period (between ~65.6 and 64.4 km). The parameter β (Figure 4f left and right panels) shows an opposite trend to that of h'. The linear fit line shows an increasing trend during both low and high solar activity periods. It is also observed that the β values are higher during low solar activity (between ~0.472 and 0.492 km^{-1}) than during high solar activity (between ~0.386 and 0.416 km^{-1}). EDD (Figure 4g left and right panels) follows a similar variation of increasing trend as of β. EDD is higher during low solar activity period (between ~16.5×10^4 and 19.0×10^4 el/cc) and lower during high solar activity period (between ~34 and 28×10^3 el/cc). In summary, it is clear that three parameters (magnitude of X-ray flux, SRAP and h') show a decreasing trend while two parameters (β and EDD) show an increasing trend, during both low and high solar activity periods. The remaining two parameters (STD and PTD) show a decreasing trend during low solar activity and an increasing trend during high solar activity.

Diurnal variation of solar flare parameters

Figure 5 shows the results of diurnal variation for the seven parameters considered here. The flares that occurred during the local day time over receiving station Prayagraj, i.e. during 0–12 UT (05:30–17:30 LT), were considered in this study. As can be seen from the figure, the maximum number of flares considered in the analysis occurred during the pre-noon time (seven out of total nine). The X-ray flux magnitude showed an increasing trend according to the linear fit line and positive slope (Figure 5a). The parameters like PTD (Figure 5d) and h' (Figure 5e) also showed an increasing trend. The remaining four parameters, namely SRAP (Figure 5b), STD (Figure 5c), β (Figure 5f) and EDD (Figure 5g), showed a decreasing trend according to the linear fit line and a negative slope. Further, these four parameters showed an overall higher value during the morning (before 10 LT).

Discussion

The diurnal and seasonal variations of the VLF signal can influence the effect of solar flares on the signal. Maurya *et al.*[3] reported that VLF amplitude also varies with TRGCP length, path direction, topography of the receiver sites, etc. Thus, in order to overcome these effects on the VLF signal,

we have used a single TRGCP (Prayagraj to NWC) throughout this study. The first X-class solar flare of solar cycle 24 occurred on 15 February 2011, with the start of solar cycle peak, and for which Lyman-α flux value was ~4.12×10^{-3} W/m^2. The Lyman-α flux values between ~3.87×10^{-3} and 4.51×10^{-3} W/m^2 during low solar activity period and between ~4.52×10^{-3} and 5×10^{-3} W/m^2 during high solar activity period were considered in this study.

Though the trend line showed a decrease in the X-ray flux during both low and high solar activity periods, the magnitude of X-ray flux was relatively higher during low solar activity period. This could be due to high X-ray flux magnitude solar flares during low solar activity periods, and it is difficult to correlate with the phase of solar activity. Further, though diurnal variations showed an increasing trend, it is clear that the magnitude of the X-ray flux is independent of any variation over the Earth.

The SRAP parameter showed similar variation as that of X-ray flux, i.e. decrease during low and high solar activity periods. There have been several studies on the correlation of X-ray flux and VLF signal amplitude change[5,12,14]. The results of these studies suggest a logarithmic relationship between VLF amplitude perturbation and solar X-ray flux. The foremost result in the present study suggests that, in general, this trend is followed during low and high solar activity variation of X-ray flux and SRAP. There are a few cases when we do not observe such a trend, e.g. in low solar activity variation for the X-ray flare event of 9 August 2011. For this X6.9 flare event, SRAP showed 4.33 dB change, while the X2.2 event, which occurred on 15 February 2011, showed a higher SRAP value (~7.83 dB). Similarly, for the X3.2 event on 14 May 2013, the SRAP value was ~5.97 dB, whereas for the X1.2 event on 15 May 2013, it was ~6.62 dB. The main reasons for these discrepancies could be seasonal and diurnal dependence of solar flare effect on the VLF signal[5]. From Figure 5b, it is clear that SRAP is maximum for the flare events that occurred during morning time (before 3UT). Also, SRAP was maximum for the events that occurred during winter. This could be related to background electron density which is low during morning and winter, and the flare effect, which is more pronounced, resulting in a higher magnitude of SRAP parameter.

The STD parameter in a few cases was zero, indicating zero-time lag between the onset of a solar flare and its effect on the VLF signal. The maximum observed STD value was 9 min. The trend line decreased during low solar activity and increased during high solar activity. This could be due to variation in the Lyman-α flux. The lower value of Lyman-α flux during low solar activity decreases the background electron density, which might affect the response of the D-region to the solar flares, and hence STD.

The PTD parameter, also called 'sluggishness' or 'relaxation time' in the literature[11], was found to be zero for five out of nine cases and 1 min for two cases. This indicates that in the case of X-class flares, due to large X-ray flux, ionization rate in the D-region is enhanced, and VLF perturbation peak, as well as X-ray flux peak, occur almost simultaneously. Here it should be noted that PTD value of zero does not indicate zero relaxation time. As the maximum resolution of X-ray flux data available on-line is 1 min, the possibility of PTD being less than 1 min cannot be ignored. For the remaining two cases PTD was found to be 5 and 6 min respectively. According to Valnicek and Ranzinger[25], PTD shows an opposite trend to that of solar ionizing radiation, i.e. PTD decreases when the solar ionizing activity increases. Grubor *et al.*[14] reported PTD value of 4 min for X1.6 class flare event, which occurred on 15 July 2004. PTD value of 6 min is possibly related to flare occurrence time (local time) and season. The local time dependence can be seen from the trend line in Figure 5d, which shows an increasing trend. In the present study, a flare of X4.9 occurred on 25 February 2014 at 00:39 UT and peaked at 00:50 UT. This period lies in the early morning part of the TRGCP, and due to the winter season, the ionosphere just started evolving, and hence a strong flare (X4.9) drastically changed the ionization rate. This could be the possible reason why relaxation took the longest time (6 min). The PTD value of 5 min appears to be a unique case, as it occurred during noon time. This might be associated with variations in the X-ray flux. Unlike other cases, the X-ray flux, in this case, peaked gradually. Thus, the VLF amplitude attained its peak slightly before the X-ray flux peak.

The D-region reflection height h' (km), decreases with an increase in the ionization of the region due to solar flares[19]. Many previous works have shown a decrease in h' value during solar flares. Thomson *et al.*[13] reported a decrease in h' of 17 km for a solar flare of X20. Most studies have reported a decrease in h' during a flare event[22]. The result of the present study indicates that h' decreases from its normal value due to variations in the X-ray flux. The average normal value of h' during the daytime was estimated as ~74 km, varying from 75 km during low solar activity to 72 km during high solar activity periods. The diurnal dependence of h' showed an increasing trend with local time, which was minimum in the morning. This is most probably due to low background electron density in the morning.

The β parameter variation shows opposite trend compared to h' parameter variation. Zigman *et al.*[12] observed an increase in β from 0.30 to 0.54 km^{-1} for a solar flare event. In the present study, the β values showed an increasing trend during both low and high solar activity periods; but it was higher than the normal day average value of ~0.30 km^{-1}. The normal day values varied from 0.28 to 0.32 km^{-1}. The β values were found relatively lower during high solar activity, trend showing an opposite thus with solar cycle. This is possible as β parameter decreases with an increase in the Lyman-α flux.

As expected, all the EDD values were positive, indicating an increase in the D-region electron density during a flare

event compared to the normal day values[11]. The estimated normal day values varied from 98 to 150 el/cm^3 with an average value of 118 el/cm^3. Further, the overall magnitude of EDD was higher during low solar activity and in the morning. This could be due to the variation of ionizing sources in the D-region, which are the Lyman-α and X-ray fluxes. The Lyman-α flux was lower during low solar activity and higher during high solar activity. This indicates that EDD is minimum when the Lyman-α flux is higher. It suggests the important role of the Lyman-α flux in the D-region ionization. For a higher magnitude Lyman-α flux, the background electron density is higher, and the solar flare effects are comparatively less pronounced; thus the EDD values are lower. A similar explanation can be given for the diurnal variation of EDD, which showed higher values during the morning. During the morning, the Lyman-α flux is lowest and starts increasing with a decrease in solar zenith angle and becomes maximum during noon when the solar zenith angle is zero. Despite the solar cycle, seasonal and diurnal variations of the D-region ionization, many sources of ionization may affect these parameters, the most notable being variation of cosmic rays, tropospheric sources, etc.[1]. It should be noted that as the number of flare cases is only nine in the present study, a quantitative conclusion cannot be made. This requires statistical analysis with more cases of X-class flares from several solar cycles. Such studies cannot be done because of limited continuous VLF data for several solar cycles from the Indian region. The results of this study are more analytical in nature and need further confirmation with solar flare events from the present and upcoming solar cycles.

Summary

The present study provides a detailed analysis of X-class flares and their impact on the low-equatorial latitude D-region ionosphere from the Indian region using NWC (19.8 kHz) VLF signal. A total of seven parameters were estimated. These parameters determine the overall effect of solar flares on the lower ionosphere/D-region and VLF propagation. The results of this study are as follows

(1) The SRAP parameter suggests a logarithmic relationship between VLF amplitude perturbation and X-ray flux, and shows a decreasing trend during both phases of the solar cycle as well as diurnal variations.

(2) The STD and PTD parameters provide approximate similar variation. A decrease during low activity and an increase during high activity is observed. Both these parameters show decreasing trends during diurnal variations

(3) The Wait parameter h' follows a variation of X-ray flux during both phases of the solar cycle and also during diurnal variations. The other Wait parameter β shows an opposite trend to that of h' and magnitude of X-ray flux.

(4) The general trend of the EDD parameter follows a variation of β during both phases of the solar cycle and diurnal variations.

We also observed that the general trend of variation, as discussed in the above four points does not follow a few individual events. This could be due to their dependence on seasonal and diurnal changes. The present study shows the initial results of the effect of the highest class (X-class) of solar flares on the lower ionosphere. Further analysis and modelling works are needed to understand the complexity of ionospheric changes during a flare event.

1. Hargreaves, J. K., *The Solar–Terrestrial Environment*, Cambridge University Press, New York, USA, 2003, p. 420.
2. Maurya, A. K., Singh, R., Kumar, S., Kumar, D. V. and Veenadhari, B., Wave-like signatures in the D-region ionosphere generated by solar flares. In Proceedings of the IEEE General Assembly and Scientific Symposium, XXXI URSI, 2014, pp. 1–4; 10.1109/URSIGASS.2014.6929796.
3. Maurya, A. K. *et al.*, Low–mid latitude D region ionospheric perturbations associated with 22 July 2009 total solar eclipse: wave-like signatures inferred from VLF observations. *J. Geophys. Res.: Space Phys.*, 2014, **119**, 8512–8523; doi:10.1002/2013JA019521.
4. Singh, R. *et al.*, D-region ionosphere response to the total solar eclipse of 22 July 2009 deduced from ELF–VLF tweek observations in the Indian sector. *J. Geophys. Res.*., 2011, **116**, A10301, 1–9; http://dx.doi.org/10.1029/2011JA016641.
5. Selvakumaran, R. *et al.*, Solar flares induced D-region ionospheric and geomagnetic perturbations in the Indian sector. *J. Atmos. Sol.–Terr. Phys.*, 2015, **123**, 102–112; doi:10.1016/j.jastp.2014.12.009.
6. Rakov, A. and Uman, M. A., *Lightning: Physics and Effects*, Cambridge University Press, New York, USA, 2006, p. 320.
7. Maurya, A. K. *et al.*, Morphological features of tweeks and night-time D region ionosphere at tweek reflection height from the observations in the low-latitude Indian sector. *J. Geophys. Res.*, 2012, **117**, A05301; http://dx.doi.org/10.1029/2011JA016976.
8. Maurya, A. K. *et al.*, Night-time D region electron density measurements from ELF–VLF tweek radio atmospherics recorded at low latitudes. *J. Geophys. Res.*, 2012, **117**, A11308; http://dx.doi.org/10.1029/2012JA017876.
9. Kumar, S., Kumar, A., Menk, F., Maurya, A. K., Singh, R. and Veenadhari, B., Response of the low-latitude D region ionosphere to extreme space weather event of 14–16 December 2006. *J. Geophys. Res.: Space Phys.*, 2015, **120**, 788–799; doi:10.1002/2014JA020751.
10. Bhatnagar, A. and Livingston, W., *Fundamentals of Solar Astronomy*, World Scientific Series, Singapore, 2005, p. 374.
11. Mitra, A. P., *Ionospheric Effects of Solar Flares*, D. Reidel Publishing Company, Dordrecht-Holland, The Netherlands, 1974, p. 220.
12. Zigman, V., Grubor, D. and Sulic, D., D-region electron density evaluated from VLF amplitude Δt during X-ray solar flares. *J. Atmos. Sol.–Terr. Phys.*, 2007, **69**(7), 775–792.
13. Thomson, N. R., Rodger, C. J. and Clilverd, M. A., Large solar flares and their ionosperic D region enhancements. *J. Geophys. Res.*, 2005, **110**, A06306; http://dx.doi.org/10.1029/2005JA011008.
14. Grubor, D., Sulic, D. and Zigman, V., Influence of solar X-ray flares on the earth ionosphere wave guide. *Serb. Astron.*, 2005, **171**, 29–35.
15. Zhang, D. H., Mo, X. H., Cai, L., Zhang, W., Feng, M., Hao, Y. Q. and Xiao, Z., Impact factor for the ionospheric total electron content response to solar flare irradiation. *J. Geophys. Res.: Space Phys*., 2011, **116**, A04311; https://doi.org/10.1029/2010JA016089.

16. Le, H., Liu, L., Chen, Y. and Wan, W., Statistical analysis of ionospheric responses to solar flares in the solar cycle 23. *J. Geophys. Res.: Space Phys*., 2013, **118**, 576–582; https://doi.org/10.1029/2012JA017934.
17. Pant, P., Relation between VLF phase deviations and solar X-ray fluxes during solar flares. *Astrophys. Space Sci.*, 1993, **209**, 297–306.
18. Bouderba, Y., NaitAmor, S. and Tribeche, M., Study of the solar flares effect on VLF radio signal propagating along NRK–ALG path using LWPC code. *J. Geophys. Res*., 2016, **121**, 6799–6807; doi:10.1002/2015JA022233.
19. Thomson, N. R., Rodger, C. J. and Dowden, R. L., Ionosphere gives size of greatest solar flare. *Geophys. Res. Lett.*, 2004, **31**, L06803; http://dx.doi.org/10.1029/2003GL019345.
20. Cohen, M. B., Inan, U. S. and Paschal, E. W., Sensitive broadband ELF/VLF radio reception with the AWESOME instrument. *IEEE Trans. Geosci. Remote Sensing*, 2010, **48**(1), 3–7; doi:10.1109/TGRS.2009.2028334.
21. Singh, R. *et al.*, Initial results from AWESOME VLF receivers: setup in low latitude Indian region under IHY2007/UNBSSI program. *Curr. Sci*., 2010, **98**(3), 398–405.
22. Clilverd, M. A., Rodger, C. J., Thomson, N. R., Lichtenberger, J., Steinbach, P., Cannon, P. and Angling, M. J., Total solar eclipse effects on VLF signals: observation and modeling. *Radio Sci.*, 2001, **36**(4), 773–788.
23. Ferguson, J. A., Computer programs for assessment of long-wavelength radio communications (Version 2.0). Space and Naval Warfare Systems Center, San Diego, CA, USA, 1998, p. 327.
24. Wait, J. R. and Spies, K. P., *Characteristics of the Earth Ionosphere Wave Guide for VLF Radio Waves*, National Bureau of Standards Technical Note, US Government Printing Office, Boulder, Colorado, 1964, p. 300.
25. Valnicek, B. and Ranzinger, P., X-ray emission and D-region 'sluggishness'. *Bull. Astron. Inst. Czechoslov*, 1972, **23**, 318–322.

ACKNOWLEDGEMENTS. The NWC (19.8 kHz) VLF data used in the work were collected by the Indian Institute of Geomagnetism, Prayagraj (http://www.iigm.res.in/) and data can be obtained for collaborative research purposes. Details of solar flares in the present work are from the National Oceanic and Atmospheric Administration, USA (https://www.swpc.noaa.gov/).

Received 6 September 2021; revised accepted 15 January 2023

doi: 10.18520/cs/v124/i7/812-819